

Resolution of concerted versus sequential mechanisms in photo-induced double-proton transfer reaction in 7-azaindole H-bonded dimer

(base pairs/photo-tautomerism)

JAVIER CATALÁN[†], JUAN CARLOS DEL VALLE[†], AND MICHAEL KASHA^{‡§}

[†]Departamento de Química Física Aplicada, Universidad Autónoma de Madrid, Cantoblanco 28049, Madrid, Spain; and [‡]Institute of Molecular Biophysics and Department of Chemistry, Florida State University, Tallahassee, FL 32306-4380

Contributed by Michael Kasha, May 27, 1999

ABSTRACT The experimental and theoretical bases for a synchronous or concerted double-proton transfer in centrosymmetric H-bonded electronically excited molecular dimers are presented. The prototype model is the 7-azaindole dimer. New research offers confirmation of a concerted mechanism for excited-state biprotonic transfer. Recent femtosecond photoionization and coulombic explosion techniques have given rise to time-of-flight MS observations suggesting sequential two-step biprotonic transfer for the same dimer. We interpret the overall species observed in the time-of-flight experiments as explicable without conflict with the concerted mechanism of proton transfer.

The doubly H-bonded dimer of 7-azaindole (7-AI) has been studied exhaustively as a model prototype for DNA base-pair tautomerization, as it is recognized to undergo a biprotonic transfer (1) on photoexcitation. A central issue in double-proton transfer (PT) reactions is whether a sequential (stepwise) or a concerted mechanism is applicable at the two proton-donor, proton-acceptor sites (2). A stepwise mechanism requires a reaction potential energy curve having an intermediate minimum between the potential minimum for the normal tautomer species, and that of the PT tautomer species, so that a finite lifetime for the transient intermediate species could be observed (3). Recent femtosecond MS results on 7-AI dimer produced in adiabatic expansion (4, 5) had been reported in supercooled molecular beams produced by adiabatic jet expansion, claiming to have established by fast transient kinetics a two-step PT mechanism for photo-excited 7-AI, with apparent theoretical calculation corroboration (6). Another laboratory (7) has made a claim of arresting the intermediate involving a one-PT in 7-AI dimer via a coulomb explosion technique, also in supercooled molecular beam experiments. We believe these results have been misinterpreted, and because they already are being accepted in some quarters (2, 8) as proven, we present refined calculations and experimental results to verify the concerted biprotonic transfer mechanism for 7-AI. Both of the jet expansion molecular beam experiments use severely invasive techniques (photoionization, coulomb explosion) to produce cationic species as required in the time-of-flight (TOF)-MS detection. We show that these laser photoionization procedures introduce a major perturbation on the electronic states of the molecular systems involved, and in effect, to create the cationic molecular species assumed to be an intermediate.

The development of femtosecond laser techniques now permits dynamic chemical events to be clocked at the picosecond and subpicosecond time scale. Consequently, a novel

duality of criteria for molecular reaction mechanisms seems to have arisen: (a) the classical requirement with demonstration of an intermediate valley in a reaction potential energy curve, or (b) a (sub)picosecond observation of passage through an intermediate molecular configuration. Both of these could satisfy the Bridgman operational criterion (9) for physical reality, if characterization of the intermediate is ascertainable and the dynamics of the reaction falls within the limits imposed by the real system. We shall compare the two possibilities for the case of biprotonic phototautomerism.

The key molecule under consideration is 7-AI (Fig. 1B), selected (1) as a prototype model for a base-pair molecule, whose double-H-bonding dimer (Fig. 1D) could serve to mimic the DNA base pairs.

Much research on the fast-time dynamics of the double-PT in 7-AI dimers has been published, starting with the pioneering picosecond domain study by Hetherington, Micheels, and Eisenthal (10). The definitive femtosecond spectroscopic study by Takeuchi and Tahara (11, 12) on the double-PT of 7-AI dimers in solution and the comprehensive spectroscopic research by Fuke *et al.* (13, 14) on high-resolution spectra of 7-AI in super-cooled jet (gaseous) neutral molecular beams offer a detailed overview of the photophysics of excitation phenomena in this molecule and its H-bonded dimer.

The initial research (1) on 7-AI established the propensity of the molecule to dimerize in a hydrocarbon solution, exhibiting a (concentration-dependent) green second fluorescence band (λ_{\max} 475 nm), which replaces the UV-violet fluorescence band (λ_{\max} 330 nm), of the monomer. The assignment of the green fluorescence to the PT tautomer of the 7-AI dimer (pyrrolo-H transferred to the aza-N, Fig. 1D) was established by comparison with the spectroscopy of the *N*-methyl stabilized PT tautomer species (7-methyl-7-H-pyrrolo[2,3-*b*]pyridine) of the 7-AI (15).

The Simultaneity Requirement

The driving force for the excited-state PT in 7-AI is the electronic rearrangement that occurs on excitation of the ground state (S_0) to the first π -electron excited state (S_1) of 7-AI. The calculated dipole moment changes from 1.61 D to 2.66 D, respectively (J.C., unpublished work), demonstrating an electronic density shift from the pyrrolo to the pyridine ring. This shift is clearly evident (Fig. 2) in the electronic distribution of the first excited molecular orbital (the now populated lowest unoccupied molecular orbital of the ground state configuration) in comparison with the electronic distribution of the highest occupied molecular orbital. This change in electronic distribution has the effect of increasing the acidity of the pyrrolo-N and simultaneously increasing the basicity of

The publication costs of this article were defrayed in part by page charge payment. This article must therefore be hereby marked "advertisement" in accordance with 18 U.S.C. §1734 solely to indicate this fact.

PNAS is available online at www.pnas.org.

Abbreviations: 7-AI, 7-azaindole; PT, proton transfer; RHF, restricted Hartree-Fock; HDF, hybrid density functional; TOF, time of flight.

[§]To whom reprint requests should be addressed.

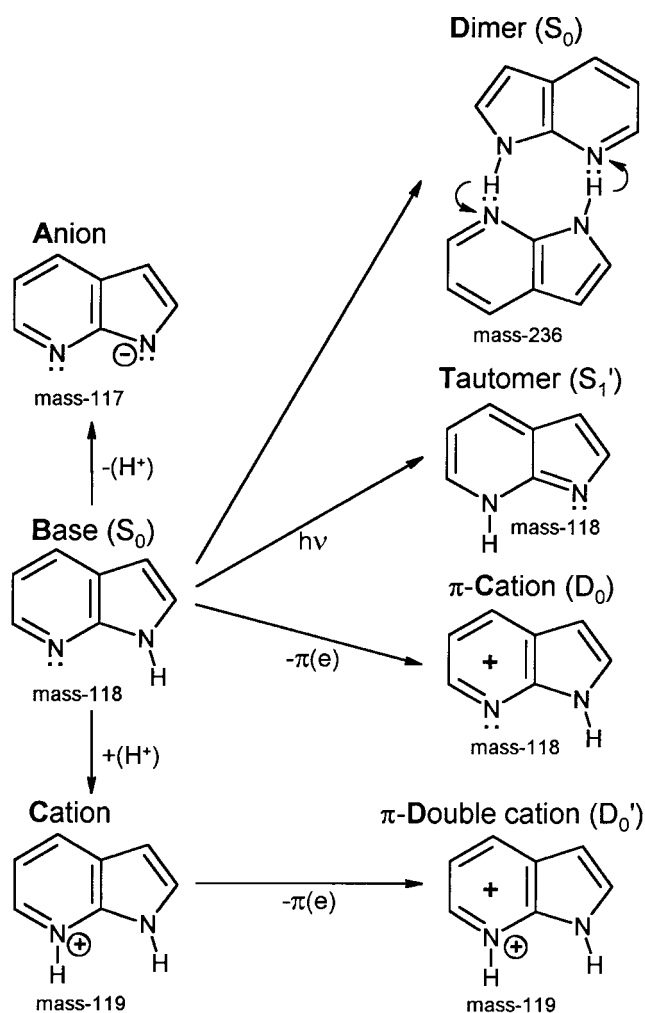


FIG. 1. 7-AI species.

the pyridino-N. In the 7-AI doubly H-bonded dimer (Fig. 1D), the two protons thus are driven to exchange their covalent bonding to the formerly H-bonded N-atom synchronously or concertedly. The characterization concertedly applies only in the case wherein both molecules are excited simultaneously to the S_1 state. The molecular orbitals for the ground state have been calculated at B3LYP/6-31G** levels with optimization of the molecular geometry. A full presentation of the calculation of charge distribution in various electronic states of 7-AI and resultant dipole moment, transition moment, and related properties will be provided elsewhere.

The possibility of simultaneous excitation of the two bases to their S_1 states was discussed in the first introduction of the 7-AI as a model molecule for DNA base-pairing (1). The simultaneous or coherent excitation of two neighboring molecules is treated by molecular exciton theory (16, 17). In the molecular exciton splitting, a vector model may be used for excited state dipole-dipole interaction, with two antiparallel transition dipoles (attractive array) representing the lower exciton state for the dimer, and two parallel transition dipoles (repulsive array) for the upper exciton state. The lower state (S_{1a} , $2A_g$) in the C_{2h} geometry of the centro-symmetric planar H-bonded dimer is strictly electric-dipole forbidden for photon absorption from the ground state (S_0 , $1A_g$). The upper exciton split level is S_{1b} , B_u and is allowed as an electric-dipole photon absorption. The key observations on the reality of molecular exciton states were the definitive observation by Fuke *et al.* (13, 14) that, indeed, there is a two-photon allowed $1A_g \rightarrow 2A_g$ ($S_0 \rightarrow S_{1a}$) electronic excitation in 7-AI H-bonded dimer (super-

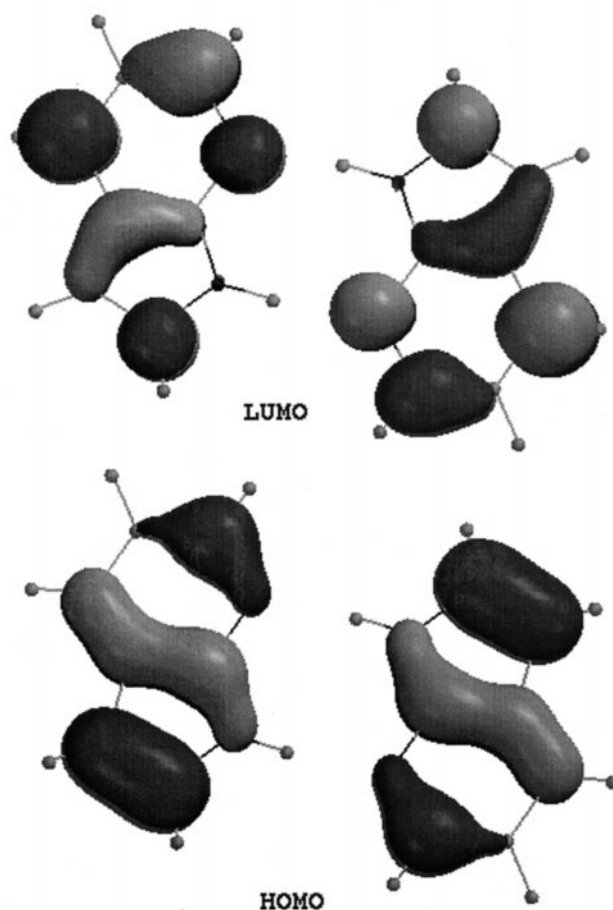


FIG. 2. Molecular orbitals for the electronic transition $S_0 \rightarrow S_{1a}$ of the 7-AI H-bonded dimer [highest occupied molecular orbital (HOMO) to lowest unoccupied molecular orbital (LUMO) excitation], showing large increase of the pyridino-N electron density. The dark vs. light shading correspond to different signs of the wave functions. The large increase in pyridino-N electron density on excitation also is seen in the second transition $S_0 \rightarrow S_{1b}$ of the 7-AI dimer.

cooled molecular beam), followed at slightly higher energy by a one-photon-allowed $1A_g \rightarrow 1B_u$ ($S_0 \rightarrow S_{1b}$) electronic excitation. This observation of a biphotonic lowest electronic transition in 7-AI dimer, followed by a normal one-photon-allowed transition, proves the existence of electronically coupled states in the dimer, i.e., that the 7-AI monomers are excited simultaneously in the dimer. As a consequence, all wave functions must be centro-symmetric for the dimer, and the driving force for concerted PT likewise should be centro-symmetric. This observation of a biphotonic absorption is the spectroscopic basis for a concerted biprotonic mechanism in the photo-excited 7-AI H-bonded dimer. In their second paper, Fuke and Kaya (14) also find a weak one-photon absorption with the same O,O origin band in the fluorescence excitation spectrum as the two-photon absorption. Those authors did not recognize the significance of their dual observations as both biphotonic and single-photon excitation. The biphotonic absorption is strong and unequivocal; a weak single-photon absorption represents a typical small relaxing of the strict exciton selection rules arising from a slight geometrical distortion of the dimer. The main component remains biphotonic for the lowest $S_0 \rightarrow S_{1a}$ transition.

The spectroscopic conditions necessary for stepwise or sequential double-PT would be as follows: For an A_1A_2 molecular 7-AI dimer in its ground state, first A_1 of the pair must be excited $A_1^*A_2$ so that the pyrrolo-H of A_2 would be

attracted to the molecule A_1^* ; then in the second step A_2 must be excited $A_1^*A_2^*$ so that the pyrrolo-H of A_1 would be attracted to the molecule A_2^* . Such an electronic mechanism is contradicted directly by excitation principles for adjacent molecules of a dimer and by extensive empirical observation.

Biprotic Transfer in Solution

The general excitonic rules prove to prevail in solution spectroscopy as well (see below). The necessity for synchronous double-PT is manifested also in tautomerization of 7-AI by protic-solvent catalysis. It was noted that simple alcohols catalyze tautomerization (1) of 7-AI, but that liquid water does not. The alcohols (e.g., methanol, ethanol) readily form a cyclical double-H-bonded solvate (1) with 7-AI, facilitating synchronous or concerted biprotic transfer by the ultrarapid mutual induction effects of the coupled proton-donor, proton-acceptor site. In liquid water, H-bonded chains and clusters would offer ample proton-acceptor and proton-donor sites, but no monomeric H_2O exists in liquid water, and the synchrony of proton-donor, proton-acceptor actions is missing. However, if monomeric H_2O is produced by micro-addition of water to a nonprotic solvent such as ethyl ether, the monohydrate cyclical complex with 7-AI readily exhibits the green fluorescence of the PT dimer (18–20). This and related experiments confirm the simultaneity requirement of concerted double-proton PT in the S_1 excited state of 7-AI. *Ab initio* calculations on aquo-complexes of 7-AI have been carried out by Shukla and Mishra (21) and independently by Chaban and Gordon (22).

Theoretical Potential Energy Curve Calculations

For quantum theoretical calculations on complex polyatomic molecules, a series of approximation methods of increasing refinement is available. For 7-AI, four levels of approximation have been used. The essentiality and methods of inclusion of electron correlation effects have been reviewed penetratingly by Raghvachari and Anderson (23).

An early all-valence electron semiempirical calculation for the PT reaction potential for 7-AI was carried out (24), by using CNDO/2 for the S_0 state geometry, followed by a configurational interaction determination of the S_1 -state Franck-Condon transition energy (CI-CNDO/2) based on the S_0 -CNDO/2 molecular orbitals. This calculation exhibited no intermediate potential minimum between the S_0 and S_1' ground state tautomer minima (normal tautomer, and 7-H PT tautomer of 7-AI, respectively), nor for the corresponding excited-state (S_1 - S_1') PT reaction potential.

Douhal *et al.* (6) have used two independent *ab initio* (nonempirical) quantum mechanical methods to investigate the potential energy curve for the PT reactions in 7-AI. (a) The first calculations used the restricted Hartree-Fock (RHF) self-consistent field technique for the ground electronic state. Electron correlation is excluded by definition in the HF procedure, the correlation energy being defined quantitatively as the energy difference between the HF energy and the true energy of a system. The HF calculation, by its limited nature, cannot be considered sufficient for studying systems that possess hydrogen bonds in their molecular structure. It is known that molecular structures involved in a PT reaction process cannot be described adequately without including electronic correlation (25). Douhal *et al.* (6) calculated the first excited singlet state reaction potential for 7-AI dimer tautomerization by using a simple configurational interaction calculation over the RHF molecular structure. (b) In a second calculation by Douhal *et al.* (6), correlation energy correction was included by using the CIS-MP2, Møller-Plesset perturbation theory taken to second order. The calculations used a 4–31G basis

set, with Gaussian-94 programs. The CIS-MP2 model is limited in its approach to full electron correlation energy and has proved unreliable in a related calculation, the potential energy surface for H-atom transfer reactions (26). The truncated basis set 4–31G is also a major limitation on the validity of the calculations presented by Douhal *et al.* (6).

The calculated reaction potential energy profiles published qualitatively (without any coordinate scales) as their figure 2 by Douhal *et al.* (6) are presented here (our Fig. 3) in corrected form. In their original form, the potential curves were shown to have an intermediate minimum. In this qualitative form, the curves have been taken as a corroboration (e.g., figure 1 in ref. 5) of the experimental results and encouraged the suggestion (7) of a two-step PT mechanism in 7-AI dimer. However, the curves drawn by Douhal *et al.* (6) do not correspond to the calculated numbers obtained by them. Introducing an energy scale on the ordinate (our Fig. 3) [based on 0–14.78 kcal/mole (min/max)] for the S_1/S_1' potential (our labels), it is obvious that there is no excited state intermediate minimum for that calculation. The Douhal *et al.* reaction potential profile (undesignated in their figure 2) seems to be for the RHF calculation, as the authors remark further in the text that the Møller-Plesset (CIS-MP-2) calculations show no intermediate minimum. It is puzzling that Douhal *et al.* (6) chose to display the results of the inadequate RHF calculation, whereas the CIS-MP-2 improved calculations would approach a more realistic potential energy curve. The transition state “humps” TS1' and TS2' shown by Douhal *et al.* (6) may not exist as they seem to depend on arbitrary introduction of geometrical distortion or on a very difficult theoretical geometry optimization.

Hybrid density functional (HDF) theory calculations were carried out for the ground electronic state in the present research, by using configurational interaction for the excited-state potential energy curve, CIS-6–31G**/B3LYP/6–31G**, with S_0 state geometry optimization. The concerted double-PT calculated potential for phototautomerism of 7-AI is given in Fig. 4. From the initial excited-state S_1 minimum (S_{1a} and S_{1b} , labeled $2A_g$ and $1B_u$) to the S_1' minimum (S_{1a}' , $1B_u$ and $2A_g'$) for the PT tautomer pair (H-bonded dimer of the 7-H tautomer) there is a single potential barrier (ca. 8.5 kcal/mol for the $2A_g$ state and 7.8 kcal/mol for the $1B_u$). These theoretical potentials confirm the absence of an intermediate minimum and reinforce the biprotic transfer mechanism in 7-AI as a concerted mechanism for simultaneous two-site bi-PT. The reliability of the HDF method is reinforced by the demonstration of reliability for an H-atom transfer reaction potential calculation (26), wherein the HDF results were preserved in the more refined quadratic configurational interaction (QCISD) calculation.

The A_g and B_u symmetries (Fig. 4) are for the centrosymmetric C_{2h} H-bonded dimer, corresponding to the excitonic split band (1) of the degenerate zero-order electronic excitonic states of the dimer pair, as discussed earlier. Analogously, HDF calculated potentials for a conjectured single PT in 7-AI dimers indicate a monotonic rise in the first PT potential from the S_1 reaction minimum (Fig. 5, *Left*), and a monotonic descent for the second PT potential to the S_1' reaction minimum (Fig. 5, *Right*). The HDF calculation yields the same symmetries and ordering of the S_1 and S_1' electronic state components as does the molecular exciton theory, without the point-dipole approximation and other limitations of the simple Davydov molecular exciton theory.

In the stable normal tautomers of 7-AI, the pyrrolo-N has a pK for proton association (Fig. 1B) at least six pK units greater than that for the pyridino-N, whereas for the excited-state PT tautomer the pK ratio is reversed, with the 7-H tautomer (Fig. 1T) being stabilized (as a fleeting transient). However, in methyl alcohol/HCl solution the cation (Fig. 1C) is readily obtainable and its absorption and fluorescence (λ_{max}

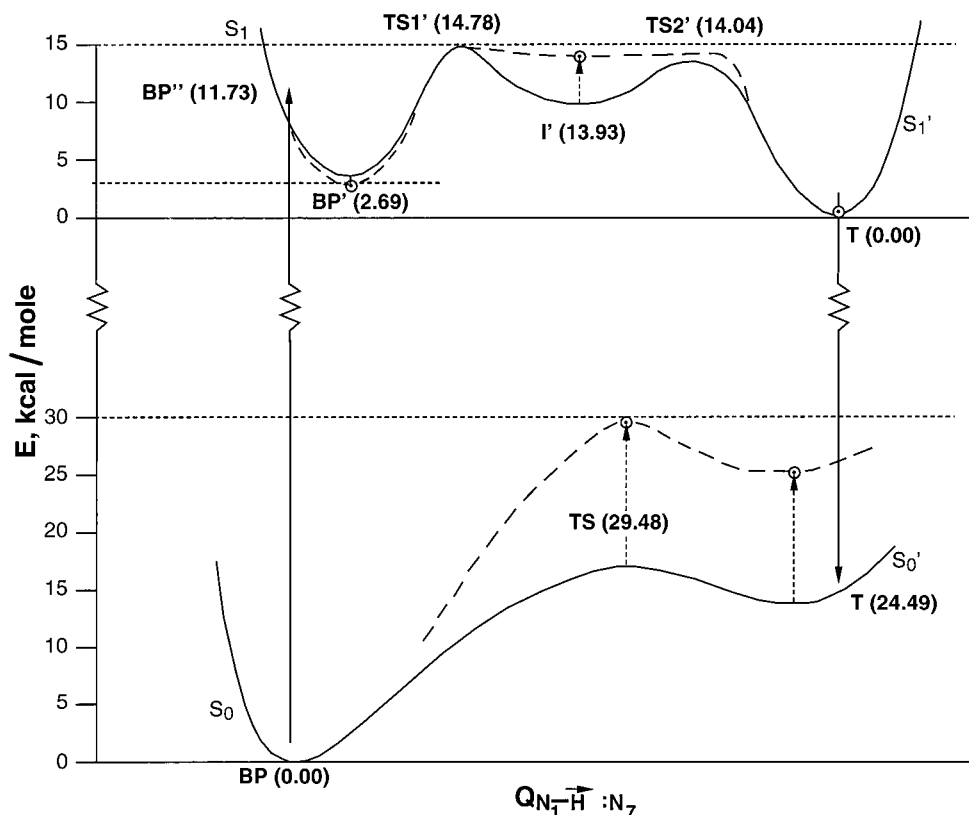


FIG. 3. PT reaction potential curves for 7-AI dimer. Solid curves as given by Douhal *et al.* (6) without scale calibration. Dashed curves corrected to correspond to published energy values of Douhal *et al.*

445 nm) spectra measured. Similarly, the analogous spectra of the anion (Fig. 1A) are observable for the DMSO/NaOH solution.

Observation of the cation (and anion) fluorescence spectra of 7-AI lying between the fluorescence bands for the neutral base 7-AI (Fig. 1B) and that for the PT-tautomer (Fig. 1T) might suggest that, e.g., the 7-AI cation (Fig. 1C) could be an intermediate single-PT species in the biprotonic transfer. This conclusion is deceptive, as a HDF calculation shows. The cation and anion (Fig. 1A) forms of 7-AI now have electronic states based on electronically perturbed molecular skeletons, which proves to be a very large perturbation. Fig. 6 presents the

energy shifts in $\text{kcal}\cdot\text{mole}^{-1}$ for the cation and anion vs. the neutral base 7-AI. Although the HDF calculation can be considered, as are all excited-state quantum theoretical calculations on large polyatomic systems, of limited precision, Fig. 6 definitely illustrates that the cation ground state (in the presence of excess acid or H^+) is so greatly lowered ($\approx 29,000 \text{ cm}^{-1}$) in energy relative to the ground state of the neutral molecule, that the cation formation would act as a trap for the double-PT if it were an intermediate. From this result, we would have to conclude that the formation of a cation as an intermediate in the excited-state double-PT is precluded in the case of 7-AI.

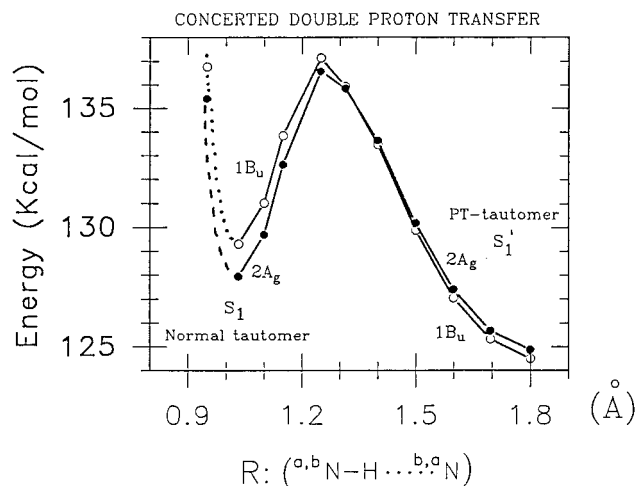


FIG. 4. Franck-Condon excited-state (S_1 – S_i) potential energy PT reaction curve for 7-AI dimer (Fig. 1D) plotted from a HDF calculation for a concerted double-PT process of the 7-AI doubly H-bonded dimer (C_{2h}).

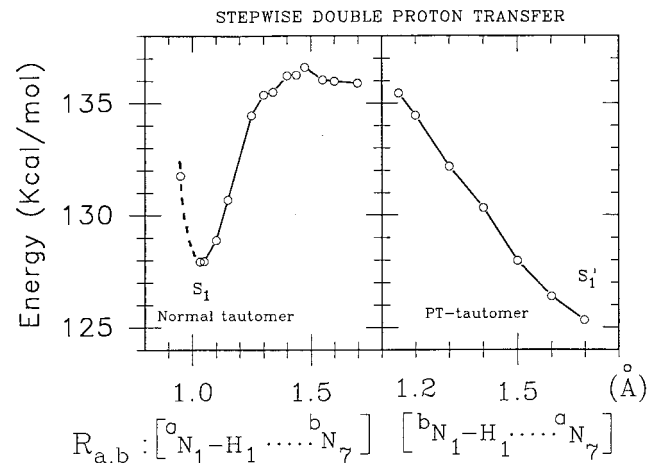


FIG. 5. Stepwise PT reaction potentials (excited states S_1 – S_i) for 7-AI dimer plotted from a HDF calculation. (Left) Transfer of first proton from pyrrolo- N_1 of lower 7-AI of Fig. 1D to pyridino- N_7 of upper 7-AI. (Right) Transfer of second pyrrolo-H of upper 7-AI to pyridino- N_7 of lower 7-AI of Fig. 1D.

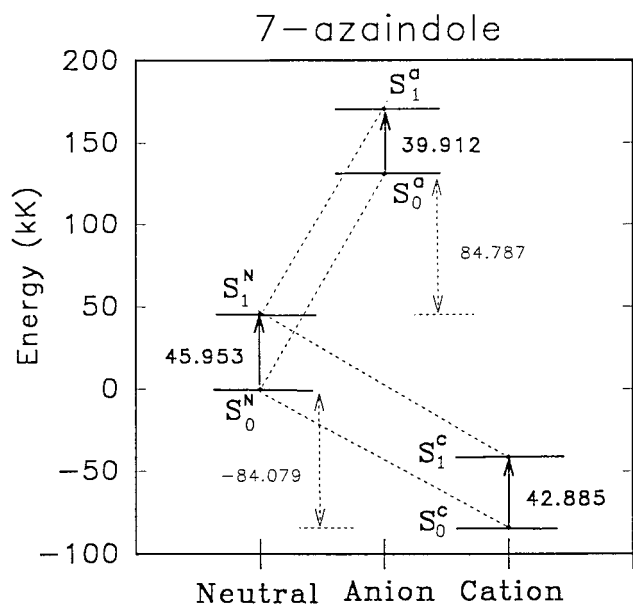


FIG. 6. Skeletal electrostatic perturbation of the π -electron states of 7-AI. HDF calculated S_0 and S_1 state energies for the 7-AI neutral base (Fig. 1B), deprotonated anion (Fig. 1A), and protonated cation (Fig. 1C).

Femtosecond Researches on 7-AI PT

We turn to an examination of the experimental researches on 7-AI by the Zewail group. In the first paper (4), an adiabatic nozzle expansion producing a super-cooled (<1 K) gaseous molecular beam is used, in the following sequence of steps: (i) adiabatic nozzle expansion of 7-AI vapor in an inert carrier gas, (ii) UV (305–310 nm) femtosecond laser pulse excitation, (iii) a second timed-delay femtosecond laser pulse (*ca.* 620 nm) yielding photoionization of the 7-AI monomers and “dimers,” with a final step (4) of TOF mass spectrometric resolution. This technique immediately raises two questions: (a) what is the nature of the dimers produced, and (b) what molecular species remain after the photoionization? In the analogous adiabatic expansion researches by the Castleman group (7), the second step involves a greatly increased intensity of the 624-nm laser pulse, yielding a coulomb explosion of the species in the excited zone of the 7-AI molecular beam.

We shall discuss briefly the complexities inherent in the TOF technique. In the ultrafast adiabatic expansion from the free jet nozzle experiment, the monomeric molecules first are thermally volatilized in the presence of an inert carrier gas in the primary chamber, then escape via the expansion nozzle. Included among the dimer structures that could form in the super-cooled (<1 K) escaping gas would be van der Waals card-pack dimers in addition to doubly H-bonded, coplanar, centrosymmetric (C_{2h}) dimers in the case of 7-AI, an additional statistical restriction arising from the severe geometrical requirement for the latter in the collisional approach. Second, the TOF technique as used (4, 5, 7) detects only (+)-charged ions. Thus (7-AI)⁺ monomers and (7-AI)(7-AI)⁺ electronically asymmetric dimers are detected, both as ion-radical species.

The outstanding result of the Castleman group research (7) was the observation of an ion-current peak for a mass-119 as a (7-AI)(H⁺) transient cation (Fig. 1C), in addition to the mass-118 normal molecule cation, 7-AI $\pi^{(+)}$, the latter arising from π -electron ionization (Fig. 1 π -C) of the companion molecule of the H-bonded dimer. The spectacular result of the coulomb explosion experiment is the extreme molecular fragmentation of a large part of the 7-AI species present: H⁺ or H₂⁺, C⁺ and numerous radical-ion intermediate fragments are

observed. The observation of simply ionized 7-AI and simply ionized (7-AI)₂ dimers (single π -electron ejection) indicates that these species happily escaped the intense coulomb explosion field. The net difference evident between the Castleman group and Zewail group research results lies actually in the much greater number of simple π -electron ionizations in the Castleman *et al.* (7) research; the coulomb explosion appears to be a destructive interference, as a side effect.

The appearance of the 7-AI(H⁺) mass-119 species (Fig. 1C) in the report of Castleman *et al.* (7) would result directly from single- π -electron ionization of those 7-AI H-bonded coplanar dimers present. This asymmetric ionization of the dimer would localize the excitation to the neutral 7-AI of the pair, the H-bond then being repelled by the 7-AI $\pi^{(+)}$ species (Fig. 1 π -C), and at the same time the pyrrolo-H of the 7-AI $\pi^{(+)}$ by its increased acidity would be readily released to the pyridino-N of the excited neutral molecule. There is then a necessity for the 7-AI(H⁺) cation to split off, leading to the observation of the mass-119, 7-AI(H⁺) species as given (7), precluding the second PT. This species would be an unstable transient with a very short lifetime. The remaining 7-AI mass-117 species is now a zwitterion: π -electron ionization leaves a (+) charge, and the pyrrolo-H dissociation a localized (−) charge; the mass-117 species cannot appear in the cation mass spectra. Thus, it appears realistic to state that the mass-119 cation observed is directly created by the photoionization detection step required by the TOF technique.

We note that a π -electron ionization of 7-AI(H⁺) species would produce the 7-AI $\pi^{(+)}$ (H⁺) double cation (Fig. 1 π -D), also not detectable in the range of the experiment. Castleman *et al.* (7) did establish the fact that the source of the 7-AI(H⁺) cation was a 7-AI dimer. However, we would indicate that the various van der Waals card-pack dimers would be stabilized by (7-AI $\pi^{(+)}$)(7-AI) dimer ionization, via ion-dipole interaction; these must be the mass-236 cations detected in the TOF mass spectra. We shall present a detailed analysis of the spectroscopy of van der Waals dimers elsewhere.

Thus, the TOF experiments of the Zewail (4) and Castleman (7) groups do not offer clear proof of intermediate single PT anion-cation 7-AI species in the PT reaction.

Supersonic jet-cooled 7-AI monomers and dimers as neutral molecular species were studied comprehensively at high-resolution electronic spectroscopy by Fuke *et al.* (13, 14). Their very detailed fluorescence and excitation spectral study established (a) the stringent need for coplanarity for double-PT in the H-bonded 7-AI dimer, (b) the dramatic effect, on PT, of the H-bond stretching mode, and (c) an electronic requirement for double-PT. The observation that the S_1 excited-state double-PT rate in 7-AI dimer was three times the rate for the H-bonded heterodimer (7-AI)(7-azacarbazole) lends support to the mutual π -electron density enhancement requirement at the 7-H proton acceptor site. This latter observation adds to the argument for a concerted double-PT. In addition, the experimentally determined PT reaction potential surface presented has no suggestion of an intermediate minimum. The theoretical study of double-PT in the centro-symmetric double-H-bonded formamide dimer parallels the demonstration of the electronic basis for a concerted biprotonic transfer (27).

A femtosecond excitation dynamics preliminary study for 7-AI dimer in solution phase indicated a rise time for biprotonic-transfer tautomer formation of 1.4 ps (28). Femtosecond excitation dynamics of double-PT in H-bonded 7-AI dimers in hydrocarbon solution at 298 K were studied in the definitive spectroscopic research by Takeuchi and Tahara (11, 12). Their observed transition times and assignments are: τ_1 , 0.2 ± 0.1 ps, $S_2 \rightarrow S_1$, internal conversion, deuterium independent; τ_2 , 1.1 ps, $S_1 \rightarrow S_1'$, PT-tautomer rise time, 1.6 ps in N-D,N-D dimer; and τ_2' , 12 ps, $S_1'(v) \rightarrow S_1'(0)$, vibrational cooling time, intramolecular vibrational relaxation.

The Zewail group (5) observed for 7-AI dimers in solution a similar range of ultrafast (0.6–0.2 ps) and a fast 1 ps (1.4–1.6 ps for deuterated N-D,N-D 7-AI dimers) transition rate. In addition, both groups observed a small component of a 12-ps slower rate. Takeuchi and Tahara (12) assigned this rate to vibrational cooling [intramolecular vibrational relaxation (IVR)] by analogy to established rates for IVR for analogous hydrocarbon molecules. The Zewail group (5) adopted the deficient RHF calculation results (6) for an intermediate reaction potential minimum (exaggerated in their figure 1) and interpreted all of their dynamics data accordingly. Takeuchi and Tahara (12) took full account of the exact 7-AI lowest molecular electronic states involved, analogous to the $S_1(L_b)$ and $S_2(L_a)$ states of iso-electronic naphthalene. Takeuchi and Tahara (12) omit the lower A_g excitonic state, preserving the upper B_u split components (1) (Fig. 3) of S_{1a} and S_{1b} , because the $S_0(1A_g) \rightarrow S_{1a}(2A_g)$ transition is electric dipole forbidden and is observed as a biphotonic transition (13, 14) as we have discussed above. As the dipole moments are rotated in plane in the PT-tautomer excited state, the A_g and B_u components reverse order (compare Fig. 4). The $S_{1a}(2A_g)$ state metastability contributes to the tautomerization dynamics and is the state from which tautomerization occurs in the dimer (13, 14).

Conclusion

The excited-state biprotonic transfer process is fundamentally spectroscopic in origin, and we have offered an outline of the principles and spectroscopic observations involved. Kinetic observations made currently by ultrafast techniques have their origin in the many molecular species produced under different excitation conditions and the complexity of the spectroscopic states that result. It was essential to unravel the several species produced in the adiabatic cooling and photoionization experiment before the kinetic isotope results could be properly correlated.

In summary we observe that (i) anionic and cationic electronic states of 7-AI are shifted strongly in energy by the skeletal charge perturbation placing them out of range as intermediates for the double-PT reaction in the neutral molecule tautomer species. (ii) High-level quantum theoretical calculations indicate a low barrier for double-PT in 7-AI with no indication of an intermediate minimum. (iii) Femtosecond dynamics and spectroscopic studies of excited-state PT reactions, with defined H-bonded centro-symmetric coplanar dimers of 7-AI, are fully interpreted without assuming an ionic intermediate via single-PT steps.

Finally, if a femtosecond/picosecond intermediate actually was detected as a natural intermediate, it would have to survive long enough to be of genetic significance as a mutation event in a DNA base pair. The maximum rate of diffusion of nucleotides to DNA polymerase is estimated (29) to be 6,000 sec^{-1} , and studies of replication rates in real biological systems (30, 31) are so far from the picosecond transient time scale as to make the ultrafast dynamical event not of genetic applicability.

We are indebted to Dirección General de Investigación Científica y Técnica of Spain for financial support. J.-C.V. is on leave from Universidad Autónoma de Madrid and thanks Florida State University for financial support.

1. Taylor, C. A., El-Bayoumi, M. A. & Kasha, M. (1969) *Proc. Natl. Acad. Sci. USA* **63**, 253–260.
2. Schowen, R. L. (1997) *Angew. Chem. Int. Engl. Ed.* **36**, 1434–1438.
3. Jencks, W. P. (1980) *Acc. Chem. Res.* **13**, 161–169.
4. Douhal, A., Kim, S. K. & Zewail, A. H. (1995) *Nature (London)* **378**, 260–263.
5. Chachisvilis, M., Fiebig, T., Douhal, A. & Zewail, A. H. (1998) *J. Phys. Chem. A* **102**, 669–673.
6. Douhal, A., Guallar, V., Moreno, M. & Lluch, J. M. (1996) *Chem. Phys. Lett.* **267**, 370–376.
7. Folmer, D. E., Poth, L., Wisniewski, E. S. & Castleman, A. W., Jr. (1998) *Chem. Phys. Lett.* **287**, 1–7.
8. Goodman, M. F. (1995) *Nature (London)* **378**, 237–238.
9. Bridgman, P. W. (1927) *The Logic of Modern Physics* (Macmillan, New York), 228 pp.
10. Hetherington III, W. M., Micheels, R. M. & Eisenthal, K. B. (1979) *Chem. Phys. Lett.* **66**, 230–233.
11. Takeuchi, S. & Tahara, T. (1997) *Chem. Phys. Lett.* **277**, 340–346.
12. Takeuchi, S. & Tahara, T. (1998) *J. Phys. Chem. A* **102**, 7740–7753.
13. Fuke, K., Yoshiuchi, H. & Kaya, K. (1984) *J. Phys. Chem.* **88**, 5840–5844.
14. Fuke, K. & Kaya, K. (1989) *J. Phys. Chem.* **93**, 614–621.
15. Robison, M. M. & Robison, B. L. (1955) *J. Am. Chem. Soc.* **77**, 6554–6559.
16. McRae, E. G. & Kasha, M. (1964) in *Physical Processes in Radiation Biology*, eds. Augenstein, L., Mason, R. & Rosenberg, B. (Academic, New York), pp. 23–42.
17. Kasha, M., Rawls, H. R. & El-Bayoumi, M. A. (1965) *Pure Appl. Chem.* **11**, 371–392.
18. Kasha, M. (1986) *J. Chem. Soc. Faraday Trans.* **82**, 2379–2392, and references therein.
19. Collins, S. T. (1982) Ph.D. thesis (Florida State University, Tallahassee).
20. Chou, P.-T., Martinez, M. L., Cooper, W. C., McMorro, D., Collins, S. T. & Kasha, M. (1992) *J. Phys. Chem.* **96**, 5203–5205.
21. Shukla, M. K. & Mishra, P. C. (1998) *Chem. Phys.* **230**, 187–200.
22. Chaban, G. M. & Gordon, M. S. (1999) *J. Phys. Chem.* **103**, 185–189.
23. Raghavachari, K. & Anderson, J. B. (1996) *J. Phys. Chem.* **100**, 12960–12973.
24. Catalán, J. & Pérez, P. (1979) *J. Theor. Biol.* **81**, 213–221.
25. Catalán, J., Palomar, J. & de Paz, J. L. G. (1997) *J. Phys. Chem.* **101**, 7914–7921, and references therein.
26. Cioslowski, J., Piskorz, P. & Moncrieff, D. (1998) *J. Am. Chem. Soc.* **120**, 1695–1700.
27. Kim, Y., Lim, S., Kim, H.-J. & Kim, Y. (1999) *J. Phys. Chem.* **103**, 617–624.
28. Share, P., Pereira, M., Sarisky, M., Repinec, S. & Hochstrasser, R. M. (1991) *J. Lumin.* **48/49**, 204–208.
29. Schlieff, R. (1993) *Genetics and Molecular Biology* (The Johns Hopkins Univ. Press, Baltimore), 2nd Ed., pp. 76–77.
30. Chandler, M., Bird, R. & Caro, L. (1975) *J. Mol. Biol.* **94**, 127–132.
31. Manor, H., Deutscher, M. & Littauer, V. (1971) *J. Mol. Biol.* **61**, 503–524.